CONTENTS

CONCEPTS

Broken mirrors: Kinetic isotope effects are excellent probes of transition structures. In this Concept, we describe recently developed kinetic isotope effect methodologies that serve to inform the symmetry-breaking process that is inherent to stereoselective reactions (see figure).

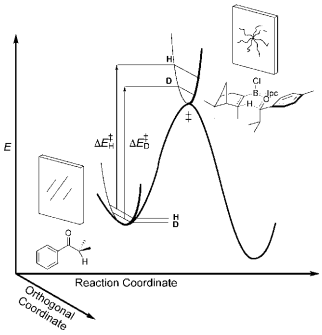

COMMUNICATIONS

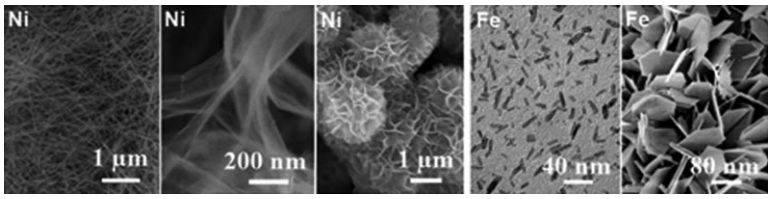

Galvanising chemistry! Galvanic replacement reactions have a very long history. However, its powerful capabilities have not been fully exploited for nanomaterial syntheses yet. Now, using very cheap, commercially available Al/Mg powders as sacrificial materials, various metals (most transition and rare earth) with a large variety of novel nanostructures can be obtained easily on a very large scale (see picture).

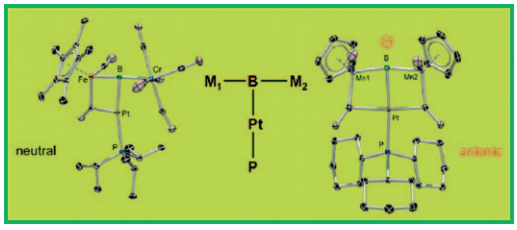

Time for T-shaped metalloborylenes: The first anionic trinuclear metal boron complex and a neutral analogue have been prepared and fully characterized. The unusual T-shaped geometry renders the title compounds, transition-metal-base-stabilized metalloborylenes, which became available by an unprecedented direct synthetic approach.

Self-Assembly

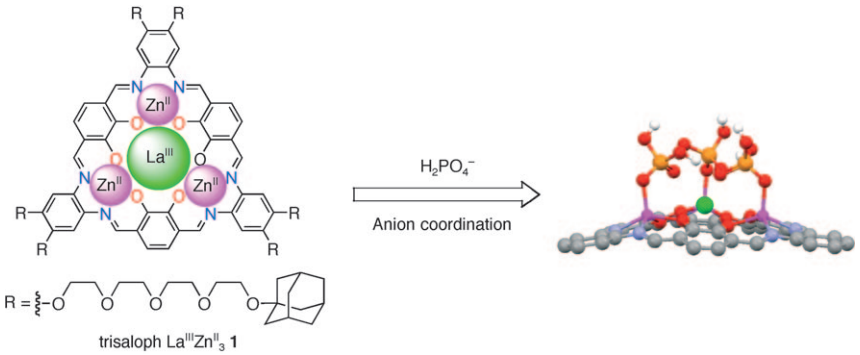

Improved solubility: Trisaloph complexes bearing PEGylated adamantane units were designed (see figure) and synthesized to improve their solubility in aqueous media. The complexes afforded a self-assembled nanostructure in aqueous media. Spherical and fibril aggregates were successfully formed based on the structural change caused by the coordinated anions.

Carboranes

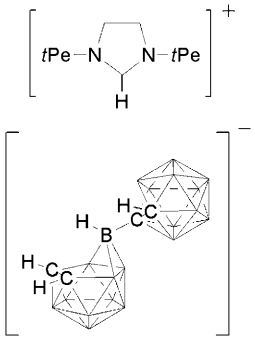

It is a matter of size: N-Heterocyclic carbenes can remove a proton from *ortho*-carborane to form a two-cage anion or attack the electropositive boron of *ortho*-carborane to yield a stable 1:2 carborane–carbene adduct. Which end product is formed depends on the steric bulk of the alkyl groups attached to the nitrogen atoms of the carbene.

Light Reactions

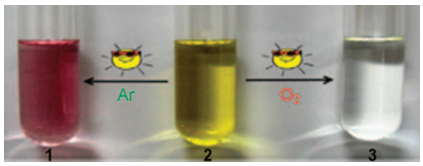

Solar conversion: Zinc hydroxyisoporphyrin (**2**), under sunlight and argon, is reduced back to zinc *meso*-tetraphenylporphyrin (**1**), but stays stable in oxygen in the absence of light. This behavior is in contrast to its iron analogue and stresses the redox role of iron in heme degradation. Compound **2** also responds to chlorophyll-type degradation (**3**) under sunlight and oxygen.

Carbon Nanotubes

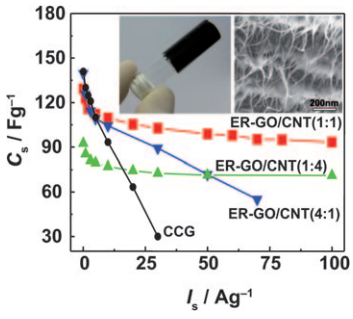

Synergistic graphenes: The chemical and electrical synergies between graphene derivatives enable a simple, cost-effective and environmentally friendly strategy for solution-phase processing of graphene oxide (GO) and carbon nanotubes (CNTs). The new nanohybrid exhibits high performance when used as electrodes for supercapacitors (see figure; ER = electrochemically reduced, CCG = chemically converted graphene).

CONTENTS

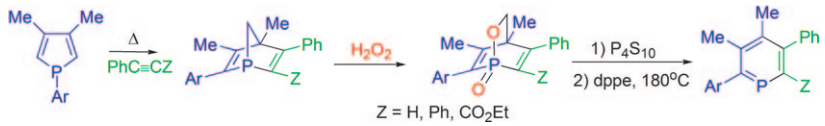

En route to phosphinines: An efficient route to convert 1-phosphanorbornadienes into phosphinines is described (see scheme). This opens up the possibiltiy to use the broad and versatile phosphole chemistry as a starting point for an equally broad variety of phosphinines.

Better together: A novel hybrid N-heterocyclic carbene (NHC) palladium complex, integrating a totally inorganic and polyanionic decatungstate unit, has been synthesized following a convergent strategy. The interplay of the Pd binding domains with the inorganic scaffold is instrumental in accessing multi-turnover catalysis in C–C cross-coupling and aromatic dehalogenation reactions under MW-assisted protocols (see scheme).

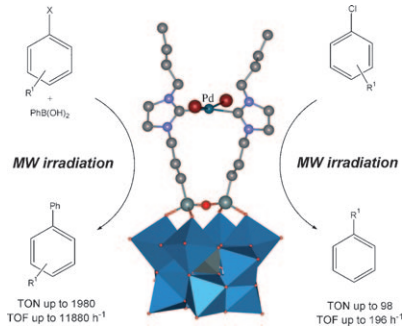

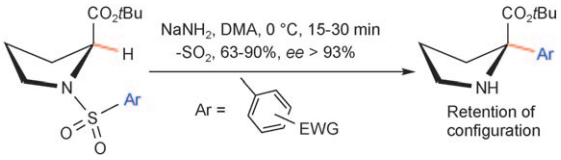

Enantiopure quaternary prolines have been prepared by stereoselective rearrangement of *N*-(arylsulfonyl)proline *tert*-butyl esters under basic conditions (see scheme), without any external source of stereochemical information. The sulfonamide aromatic ring must contain an electron-withdrawing group (EWG), which stabilizes an intermediate Meisenheimer complex. The overall process provides easy entry to a series of optically pure α-aromatic prolines.

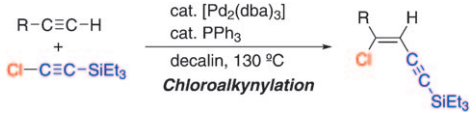

Useful intermediates: Addition of silyl-substituted chloroalkynes to terminal alkynes, namely chloroalkynylation, proceeds under palladium catalysis to afford (*Z*)-1-chloro-1,3-enynes (see scheme). The carbon–chlorine bond of the adducts is easily convertible to a carbon–carbon bond by using palladium-catalyzed cross-coupling reactions to provide a variety of 1,3-enynes.

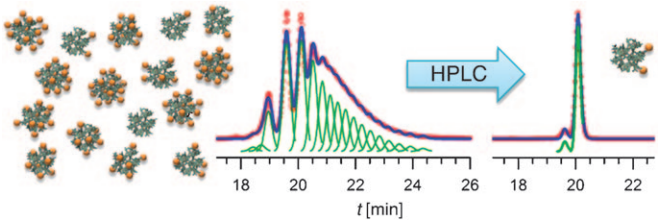

Precision dendrimer: Nine different dendrimer components with precise numbers of a functional ligand were isolated leading to an order of magnitude improvement in the purity of each component.

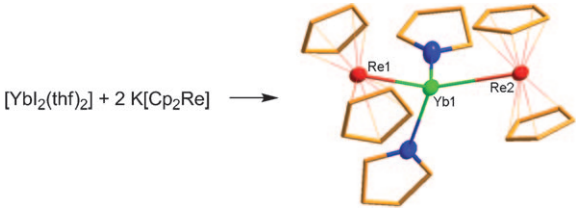

Salt of the (rare) earth: The reactions of ytterbium(II) iodide with alkali metal salts of the [CpRu(CO)$_2$] and [Cp$_2$Re] anions afford molecular compounds that have two unsupported Yb–TM bonds (TM = transition metal; see scheme). Electron localisability indicator calculations were performed and revealed highly polar metal–metal bonds.

FULL PAPERS

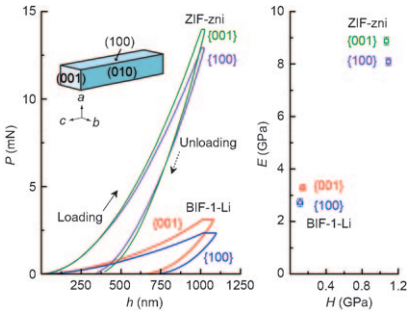

Dense ZIFs: Two topologically identical hybrid frameworks possess similar bulk moduli, yet strikingly different elastic moduli and hardnesses. The role of the inorganic species in each framework is scrutinised, with results drawn on the dominant factors involved in their mechanical response (see graphic). The results have far-reaching implications in the design of new hybrid materials, whilst explaining previous anomalies.

CONTENTS

Minimal but hyper: One single mutation of FucA aldolase (F131A) extends its acceptor substrate tolerance to bulky and conformationally restricted *N*-Cbz-amino aldehydes (Cbz = benzyloxycarbonyl), including (*R*)-*N*-Cbz-prolinal, for which no detectable activity was observed with the FucA wild type. FucA F131A was an excellent catalyst for the aldol addition of dehydroxyacetone phosphate to hydroxyprolinal derivatives (see figure), leading to novel polyhydroxylated pyrrolizidines related to the hyacinthacine and alexine types.

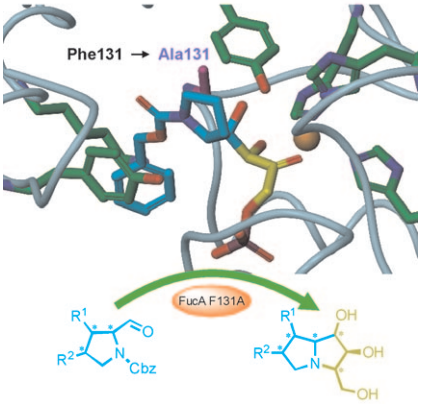

Cancer measures up: Electrochemical and electrochemiluminescence cytosensors for the detection of Ramos cells has been developed by taking advantage of the easy separation of magnetic beads and the high affinity of aptamers with and without amplification of the nanoparticles (see figure).

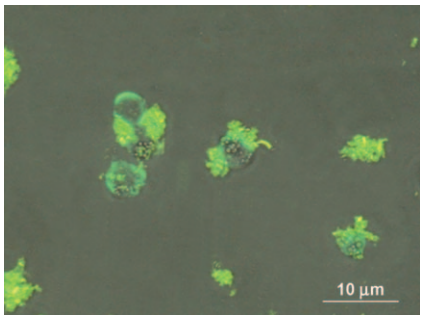

Sugar recognition and allergies: A combined approach of NMR spectroscopy and molecular modeling (see figure) has permitted us to deduce the structure of Asn-linked Man(GlcNAc)$_2$ bound to hevein. Given the ubiquity of the Man(GlcNAc)$_2$ core in all mammalian *N*-glycoproteins, the basic recognition mode presented herein might be extended to a variety of systems with biomedical importance.

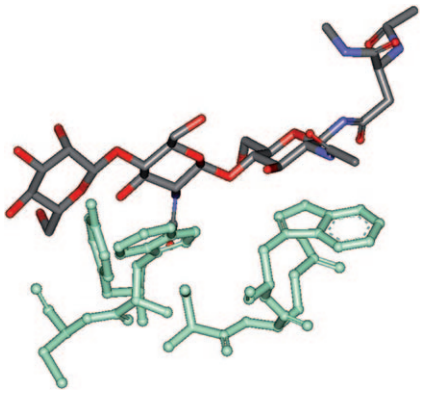

Just relax! Three different Gd^{III} complexes were anchored on the surface of MCM-41 silica nanoparticles functionalised with $-NH_2$ groups. The porous support markedly influences the magnetic properties of the Gd^{III} chelates. The dramatic relaxivity enhancement observed after acetylation of the amino groups (see figure) results in an extremely high magnetic resonance imaging (MRI) sensitivity per particle.

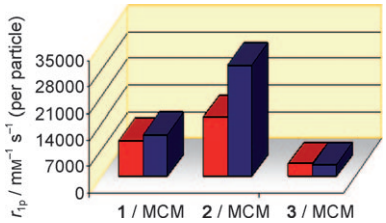

Nanoparticles

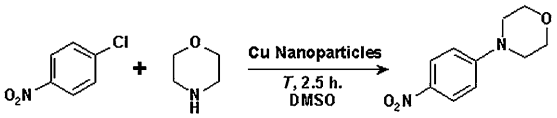

Control the shape: Copper nanoparticles with tunable sizes and shapes were synthesized by reducing copper(II) salt with hydrazine in an aqueous solution that contained poly(acrylic acid) (PAA) as the capping agent. Cuboctahedron-shaped copper nanoparticles were readily obtained by adjusting the concentration of PAA. Among other applications, they have shown significant catalytic activity and selectivity in C–N coupling (see scheme).

Supramolecular Assembly

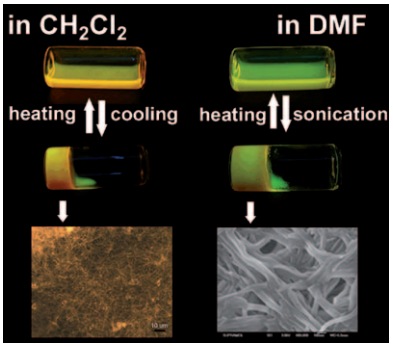

Instant gel: Two novel urea-functionalized quinacridone derivatives have been designed and synthesized, and multi-stimuli-responsive organogels based on these smart materials have been obtained. Environmental factors, such as temperature and sonication, can effectively tune their supramolecular assembly properties (see figure) and provide a deep understanding of the mechanism of stimuli-responsive gelation.

Nanomaterials

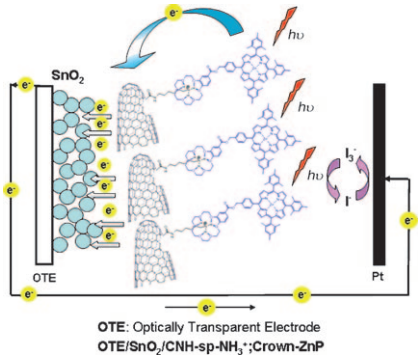

Around the horn: A new light-sensitive nanohybrid based on a carbon nanohorn (**CNH**) and a zinc–porphyrin bearing a crown ether group (**CNH**-sp-NH_3^+;Crown–ZnP) has been prepared by a relatively simple self-assembly procedure. Photoinduced electron-transfer processes of the nanohybrids are confirmed, and the moderate efficiency of this system in photovoltaic solar cells is shown.

Quantum Dots

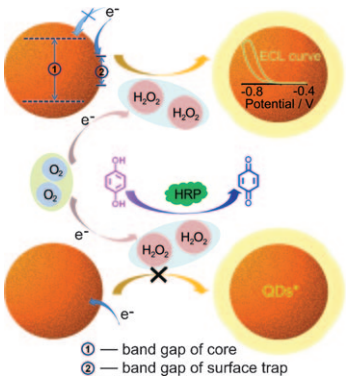

A narrow surface band gap and low-potential electrochemiluminescence (ECL) of quantum dots (QDs) were achieved by using dithiol compound as a stabilizer to form surface traps on the QDs. H_2O_2 produced from the reduction of dissolved oxygen was demonstrated to be the co-reactant of the cathodic ECL process, which could lead to the extensive application of the QDs in ECL biosensing for peroxidase-related analytes.

CONTENTS

Unseen power of the picket fence: A biofunctional nanocomposite of reduced graphene oxide (RGO) with water-soluble picket-fence iron porphyrin (FeTMAPP) has been prepared through π–π interactions (see image). It has good biocompatibility and dispersion in water, and shows fast electronic communication between the porphyrin plane and flattened RGO for chlorite reduction.

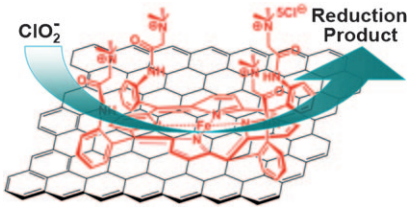

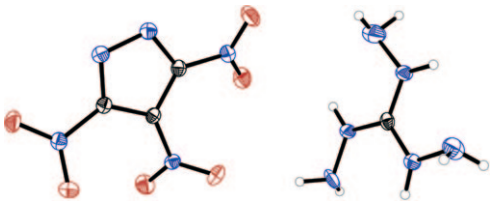

Out with a bang! From the calculated detonation pressure (23.74–31.89 GPa) and velocity (7586–8543 ms^{-1}), 3,4,5-trinitropyrazolate salts have potential as energetic materials. Impact sensitivities were determined to be no less than 35 J by hammer tests, which placed these salts in the insensitive class.

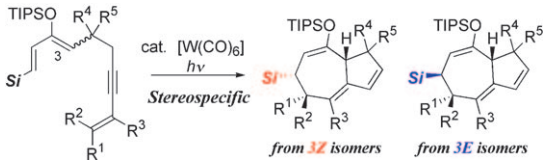

Tungsten-catalyzed tandem cyclization of 3-siloxy-1,3,9-triene-7-yne derivatives allowed stereoselective preparation of a variety of synthetically useful functionalized bicyclo[5.3.0]decane derivatives (see scheme). This reaction should provide a powerful method for the synthesis of natural products with a bicyclo[5.3.0]decane framework from easily available acyclic precursors. ***Si*** = Me_2PhSi, TIPS = iPr_3Si.

Fullerenes: A series of truly water-soluble and tightly coupled porphyrin/C_{60} electron-donor–acceptor conjugates (see figure) have been synthesized, in which the charge-separation and charge-recombination dynamics are controlled by modifying the nature of the dendrimer and/or the choice of the central metal atom.

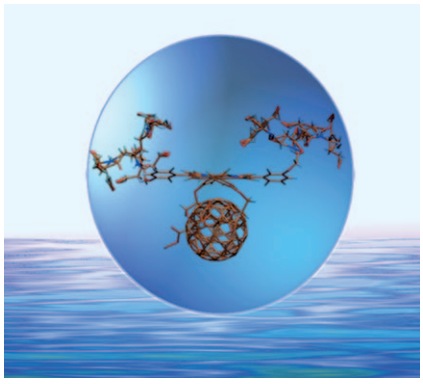

Sigma-Acceptor Ligands

silanes as σ-acceptor ligands

Metal→silane interactions: Coordination of ambiphilic diphosphine–silane ligands *o*-[(*i*Pr$_2$P)C$_6$H$_4$]$_2$SiRR′ to AuCl affords pentacoordinate neutral silicon compounds in which the metal center acts as a two-electron donor and the silane as a σ-acceptor ligand (see picture). Spectroscopic, structural, and theoretical data substantiate the influence of the substitution pattern at silicon on the Au→Si interaction.

Organometallic Anion Hosts

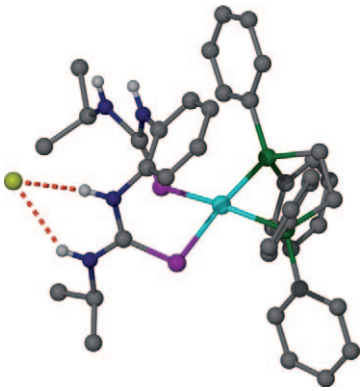

Unusual bindings: Treatment of a range of bis(thiourea) ligands with inert organometallic transition-metal ions gives a number of novel complexes that exhibit unusual ligand binding modes and significantly enhanced anion binding ability.

Pt SALDI Substrates

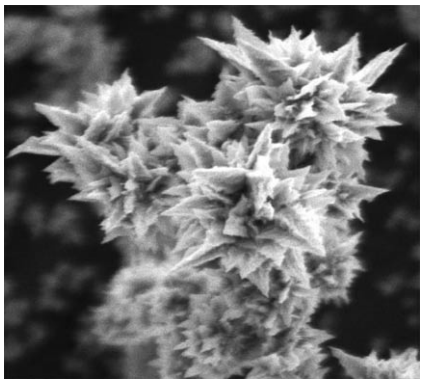

Platinum nanoflowers: We report a new and facile method for synthesizing three-dimensional (3D) platinum nanoflowers (Pt Nfs) on a scratched silicon substrate by electroless galvanic displacement (see SEM image). The Pt Nf silicon hybrid plate shows excellent surface-assisted laser desorption/ionization (SALDI) activity.

Catalyst Activation

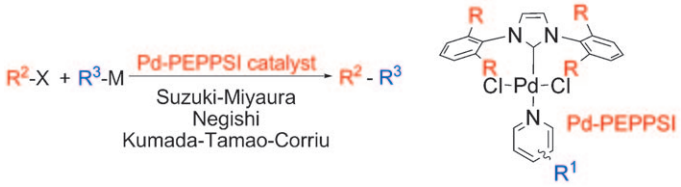

Get active! An array of N-heterocyclic carbene and pyridine ligands were evaluated in a wide variety of coupling reactions to probe the activation of the Pd–PEPPSI (pyridine, enhanced, precatalyst, preparation, stabilisation and initiation) catalyst (see scheme).

CONTENTS

* Author to whom correspondence should be addressed

Supporting information on the WWW (see article for access details).

VIP Full Papers labeled with this symbol have been judged by two referees as being "very important papers".

A video clip is available as Supporting Information on the WWW (see article for access details).

SERVICE

Issue 34/2010 was published online on September 6, 2010

CORRIGENDUM

*K. Ahlford, J. Ekström, A. B. Zaizsev, P. Ryberg, L. Eriksoon, H. Adolfsson**..... 11197–11209

Asymmetric Transfer Hydrogenation of Ketones Catalyzed by Amino Acid Derived Rhodium Complexes: On the Origin of Enantioselectivity and Enantioswitchability

Chem. Eur. J., **2009**, *15*

DOI: 10.1002/chem.200900548

In their Full Paper, the authors have found that the CCDC number in reference [17], which contains crystallographic data of the rhodium complex presented in Figure 2, is unfortunately incorrect. The correct CCDC number is 736138 and not 712178. The authors sincereley apologize for this error and any inconvenience it may have caused.

